

PLANAR DIAGRAMS FOR LOCAL INVARIANTS OF GRAPHS IN SURFACES

CALVIN MCPHAIL-SNYDER AND KYLE A. MILLER

ABSTRACT. In order to apply quantum topology methods to non-planar graphs, we define a planar diagram category that describes the local topology of embeddings of graphs into surfaces. These *virtual graphs* are a categorical interpretation of ribbon graphs. We describe an extension of the flow polynomial to virtual graphs, the S -polynomial, and relate it to Penrose polynomials. The S -polynomial is used to define an extension of the Yamada polynomial to virtual spatial graphs, and with it we obtain a sufficient condition for non-classicality of virtual spatial graphs. We conjecture the existence of local relations for the S -polynomial at squares of integers.

1. INTRODUCTION

The study of invariants of topological objects like knots and links can frequently be simplified by the use of diagram categories. These are categories whose objects are intervals with marked points and whose morphism spaces are of diagrams drawn between them, for example of graphs or tangles. Numerical invariants of these objects correspond to functors from these categories to simpler, linear categories with local relations. Perhaps the most famous example is the use of the Kauffman bracket (equivalently, the \mathcal{R} -matrix of $\mathcal{U}_q(\mathfrak{sl}_2)$) to construct the Jones polynomial.

Many of the examples in the literature correspond to diagrams drawn in the plane, such as the tangle diagrams used in Reshetikhin-Turaev invariants [21]. Similarly, in [10] Fendley and Krushkal consider a category of planar graphs whose vertices are of degree 3 (cubic graphs). An obvious generalization is to ask what happens when the objects are nonplanar. For example, one might be interested in colorings of graphs on tori instead of the plane. The diagrams of the relevant category are no longer drawn in the plane, but instead on a compact oriented surface with boundary, as in Figure 1, and analyzing composition laws can become more difficult. In this paper, we explain how

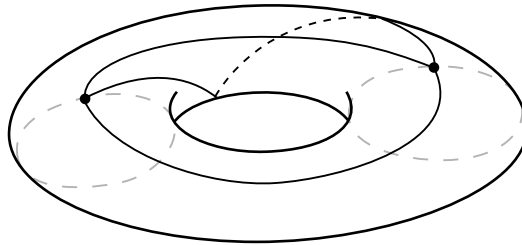


FIGURE 1. The theta graph Θ_3 cellularly embedded in a torus.

to represent the local information of graphs on surfaces in terms of planar diagrams for objects we call *virtual graphs*, named so for their suitability for representing diagrams for virtual links and virtual spatial graphs. Virtual graphs are equivalence classes that unite the notions of ribbon graphs and cellular embeddings.

One perspective on our construction is as follows: When considering invariants of planar graphs or similar objects, it makes sense to adopt a functional or categorical viewpoint. Graphs drawn in planar surfaces with boundary can have edges incident to the boundary, and these boundary

Date: April 2018.

edges can be glued to the boundary edges of other such diagrams. This idea can be formalized in a number of ways, such as planar algebras, operads, or tensor categories.

It is then natural to ask what happens when the graphs are instead embedded in arbitrary surfaces. A formalization is to consider a decorated $(1+1)$ -dimensional oriented cobordism category: objects are closed 1-manifolds (circles) with marked points, and morphisms are oriented cobordisms between them, decorated with embedded graphs meeting the marked boundary points in half-edges. We refer to such graphs as *surface graphs*, and in Definition 4.3 we give a variation, the *stable surface graph category*, where we impose the structure of a symmetric monoidal category.

From this perspective, the data of a numerical invariant such as the flow polynomial, the Penrose polynomials, or the S -polynomial of Definition 3.3 corresponds to a monoidal functor (possibly with other properties) from the surface graph category to the category of vector spaces. Such a functor is a type of $(1+1)$ -dimensional topological quantum field theory. These theories are most naturally described in terms of diagrams drawn on surfaces, and like in the situation of knots, links, and tangles, for many purposes it is easier to work with projected two-dimensional planar diagrams. We use the viewpoint of virtual graphs to study invariants that naturally respect the symmetric monoidal structure.

In the following, all surfaces are compact and oriented, possibly with boundary. Assume all embeddings are with respect to the PL topology.

2. VIRTUAL GRAPHS AND VIRTUAL SPATIAL GRAPHS

In this section we define *virtual graphs*, which provide a planar calculus for the local information of graphs embedded in surfaces. The motivation for these virtual graph diagrams is to extend objects like the flow category in [1] to non-planar graphs, to define a Temperley-Lieb-like category for surfaces, and to give a setting for objects such as 3-graphs [8], or (4-valent) virtual graphs and the category *GraphCat* of cubic graphs from [14]. Virtual graphs are represented by objects frequently called *combinatorial maps* or *ribbon graphs*, but we wish to emphasize the topology and de-emphasize a particular surface embedding.

We define *virtual spatial graphs* as virtual graphs with special 4-valent vertices for classical crossings subject to Reidemeister moves, instead of using Gauss codes as in [11], and we review the interpretation of virtual spatial graphs as ribbon graphs embedded in thickened surfaces.

2.1. Virtual graphs. By a *graph* we mean a compact 1-dimensional CW complex, which in other words is a finite abstract graph topologized so its vertices are points and its edges are closed unit intervals.

Definition 2.1. A *surface graph* $G \hookrightarrow \Sigma$ is a graph G embedded in the interior of a compact oriented surface Σ , possibly with boundary.

There are two special kinds of surface graphs $G \hookrightarrow \Sigma$:

- (1) A surface graph is a *cellular* or *combinatorial* embedding if $\Sigma - \nu(G)$ (the complement of a regular neighborhood) is a disjoint union of closed disks.
- (2) A surface graph is a *ribbon graph* if $G \hookrightarrow \Sigma$ is a homotopy equivalence.

Cellular embeddings have, up to isotopy, a well-defined (*geometric* or *Poincaré*) *dual* surface graph $G^* \hookrightarrow \Sigma$ made by placing a single vertex inside each disk of $\Sigma - \nu(G)$ and joining such vertices by an edge when the corresponding disks are adjacent to the same edge of G . In particular, the edges of G and G^* are in one-to-one correspondence, and we can arrange for each dual pair to transversely intersect at a single point. This is the usual dual graph in the case of a graph embedded in the plane.

Cellular embeddings and ribbon graphs are intimately related. Given a cellular embedding $G \hookrightarrow \Sigma$, the restriction $G \hookrightarrow \text{cl}(\nu(G))$ is a ribbon graph. Conversely, given a ribbon graph $G \hookrightarrow \Sigma$, the extension $G \hookrightarrow \Sigma'$ obtained by gluing disks into the boundary of Σ to obtain a closed manifold Σ'

yields a cellular embedding. Up to composition with a surface homeomorphism, these are inverse operations.

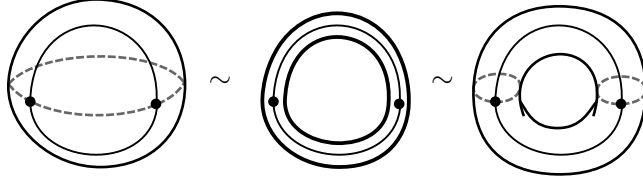


FIGURE 2. Example of stable equivalences, where the annulus in the middle is embedded in a sphere (left) and a torus (right).

Definition 2.2. Suppose $G \hookrightarrow \Sigma$ is a surface graph and A *stabilization move* of a surface graph $G \hookrightarrow \Sigma$ is the surface graph given by the composition $G \hookrightarrow \Sigma'$, where $\Sigma \hookrightarrow \Sigma'$ is an orientation-preserving embedding into a compact oriented surface Σ' . *Stable equivalence* is the equivalence relation on surface graphs generated by isotopy and stabilization moves. See Figure 2.

This definition is analogous to the one for virtual link diagrams in [6]. The closed surface representatives are all related by 0-surgery and 1-surgery in the complement of G .

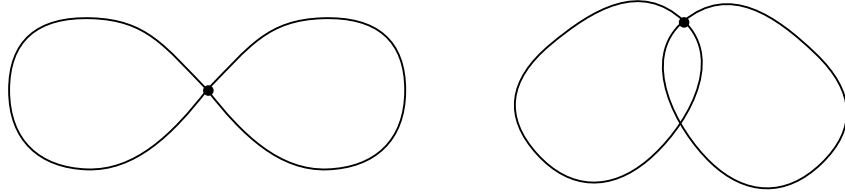


FIGURE 3. Planar and nonplanar virtual graphs.

Stable equivalence allows us to ignore irrelevant topology. For example, any planar graph can be embedded in a disk that is itself embedded in a surface of higher genus, yet locally the graph is still essentially planar. This sort of situation arises naturally when considering categories whose morphisms are represented by formal linear combinations of surface graphs with edges incident to the boundary, and stable equivalence is what will allow us to form a symmetric monoidal category. Furthermore, edge deletion becomes as simple as restricting the surface graph to a subgraph.

Definition 2.3. A *virtual graph* is a stable equivalence class $[G \hookrightarrow \Sigma]$ for a surface graph $G \hookrightarrow \Sigma$. By abuse of notation, we call G the virtual graph.

Every virtual graph can be represented by a ribbon graph by destabilizing an arbitrary representative surface graph to a closed regular neighborhood of the graph.

The data for an arrow presentation of a ribbon graph may also be given by the counterclockwise cyclic ordering of the half-edges of G incident to each vertex, the totality of which is called a *rotation system* for G . Specifically, following [8], with \mathcal{H} being a finite set (of half-edges), let $\alpha, \sigma \in \text{Sym}(\mathcal{H})$ be permutations such that the orbits of α are all of size 2. The orbits of α and σ respectively give the edges and vertices of a graph, and σ is its rotation system.

A virtual graph can be specified by a *virtual graph diagram*, which is an immersion of a graph G in the plane such that (1) no two vertices coincide, (2) no vertex coincides with the interior of an edge, and (3) edges intersect transversely. Such intersections are called *virtual crossings*. One may imagine that the diagram portrays the image of G through an orientation-preserving planar immersion of a ribbon graph representative.

The rotation system is obtained from such a diagram by reading off the half edges incident to a vertex in counterclockwise order. Virtual graphs are in bijective correspondence with virtual graph diagrams up to isotopy, modulo the moves in Figure 4. As an example, the two virtual graphs in Figure 5 have the same underlying graph but different rotation systems, and hence are inequivalent.

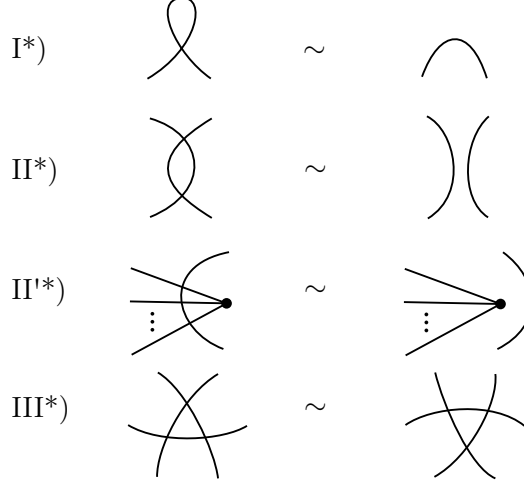


FIGURE 4. Diagrammatic moves for virtual graph equivalence.

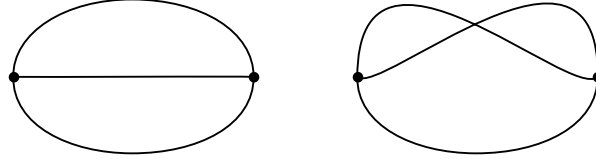


FIGURE 5. Two inequivalent virtual graphs whose underlying graph is the *theta graph* Θ_3 . The second is represented by the surface graph in Figure 1.

One can also obtain a representative surface graph from a virtual graph diagram by a straightforward construction that preserves the rotation system: replace a small disk neighborhood of each virtual crossing by a punctured torus with the edges routed so they no longer cross. This construction is illustrated in Figure 6.

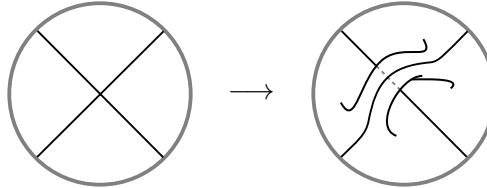


FIGURE 6. Resolving a virtual crossing by a connect sum with a torus.

As a first invariant, the *genus* of a virtual graph G is

$$g(G) = \min_{G \hookrightarrow \Sigma} g(\Sigma),$$

where $g(\Sigma)$ is the sum of the genera of the connected components if Σ is disconnected. In particular, if $G \hookrightarrow \Sigma$ is a cellular embedding, $g(G) = g(\Sigma)$. A *planar* virtual graph is one whose genus is zero,

and an abstract graph is planar if and only if it is the underlying graph of some planar virtual graph. Virtual graphs up to move VI* in Figure 11 are the same as abstract graphs.

With G a virtual graph and $G \hookrightarrow \Sigma$ a representative cellular embedding, the dual virtual graph G^* is defined to be the dual $G^* \hookrightarrow \Sigma$ as a virtual graph.

2.2. Virtual spatial graphs. A *spatial graph* G is an embedding of a ribbon graph $G \hookrightarrow \Sigma$ in S^3 , where Σ is the *ribbon structure* of the spatial graph. The data of a spatial graph can be given by a link diagram extended to represent the vertices of G . The ribbon structure of G can be read off from such a diagram through the so-called blackboard framing, where the diagram is thought of as the image of G through an orientation-preserving immersive projection of a ribbon graph onto the equatorial S^2 . (This is the most restrictive definition for a spatial graph with unoriented edges, where the diagrams are up to *rigid vertex isotopy* and *regular isotopy*. The least restrictive, an embedding of the graph itself, is up to *pliable vertex isotopy* and the full set of Reidemeister moves. See [24] and [11].)

The combinatorial data of a spatial graph diagram is a virtual graph with distinguished 4-valent *classical crossings* marked with which pair of opposite incident half edges corresponds to the over-strand. By disregarding the planarity of the diagram, we obtain *virtual spatial graphs*. This is equivalent to the approach in [11], which extends the original Gauss code approach for virtual links in [13] to define virtual spatial graphs.

Virtual spatial graphs are related by the virtual graph moves in Figure 4, where II'^* applies to the classical crossings as well (illustrated in Figure 7), along with the Reidemeister moves for links up to regular isotopy in Figure 8 and the moves for rigid vertex isotopy in Figure 9.



FIGURE 7. How move II'^* applies to classical crossings.

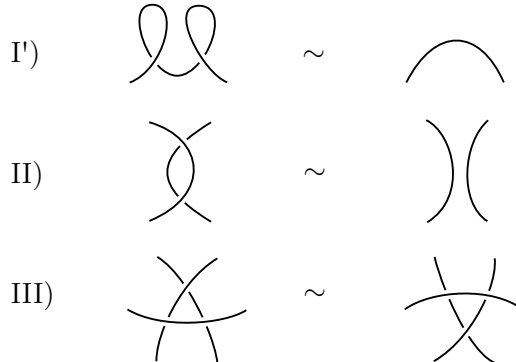


FIGURE 8. Reidemeister moves for links up to regular isotopy.

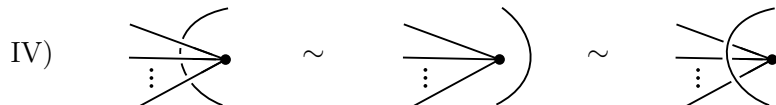


FIGURE 9. Moves for rigid vertex isotopy.

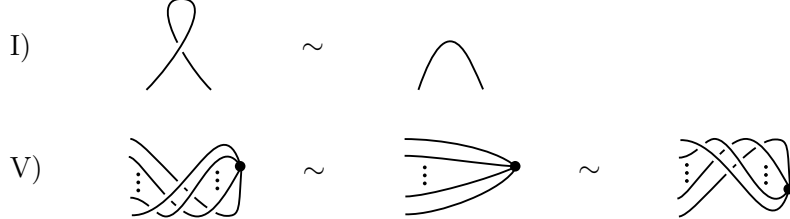


FIGURE 10. Moves for rigid vertex isotopy for *flat vertex graphs*, spatial graphs whose edges are not framed and whose vertices are unoriented disks.

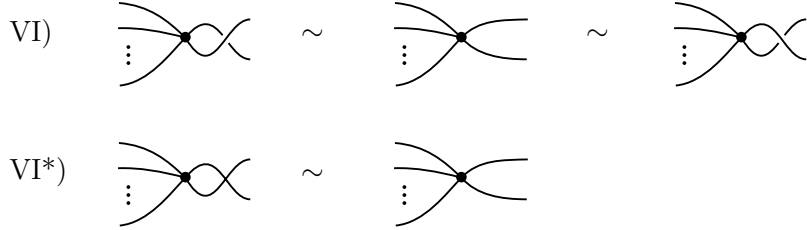


FIGURE 11. Moves for pliable vertex isotopy (VI) and virtual pliable vertex isotopy (VI*).

Being a virtual graph, a virtual spatial graph can be represented as a surface graph $G \hookrightarrow \Sigma$ with distinguished 4-valent vertices for classical crossings. That is, a spatial graph diagram on a compact surface. By thickening the surface Σ and teasing apart the classical crossings, we may obtain a ribbon graph embedding $G \hookrightarrow \Sigma \times I$ from the blackboard framing, where $I := [0, 1]$. The definition of stable equivalence extends to thickened surfaces by requiring that the stabilization move $\Sigma \times I \hookrightarrow \Sigma' \times I$ be induced from a map $\Sigma \hookrightarrow \Sigma'$.

Theorem 2.4. *Virtual spatial graphs are in bijective correspondence with ribbon graphs in thickened closed oriented surfaces modulo stable equivalence. Furthermore, each has a unique representative in a thickened closed surface of minimal genus, up to self-homeomorphism induced by orientation-preserving self-homeomorphism of the surface.*

Proof. The fact that virtual spatial graphs correspond to spatial graph diagrams on compact surfaces up to stable equivalence is a result of Carter, Kamada, and Saito [6]. Kuperberg applied JSJ theory to characterize the unique minimal representative, where minimality is in the sense that every properly embedded annulus in the graph complement that connects the two boundary components of the thickened surface bounds a ball [17]. \square

In particular, once a virtual graph is represented as a diagram on a minimal-genus closed surface, equivalence is completely generated by the moves for regular isotopy and rigid vertex isotopy, along with the action by the mapping class group. The *virtual genus* of a virtual spatial graph is the genus of this surface. A consequence of Theorem 2.4 is that if two spatial graphs are equivalent as virtual spatial graphs, they are indeed equivalent as spatial graphs.

Corollary 2.5. *Let G be a virtual graph. The virtual genus of G as a virtual spatial graph equals the genus of G .*

Proof. Consider a cellular embedding $G \hookrightarrow \Sigma$ of a non-planar virtual graph, and consider an extension to $G \hookrightarrow \Sigma \times I$ by composition with $x \mapsto (x, \frac{1}{2})$. Let $A \subset \Sigma \times I$ be a properly embedded annulus in the complement of G connecting the two boundary components of $\Sigma \times I$. Consider the intersection between A and $\Sigma_0 = \Sigma \times \frac{1}{2}$, which is a collection of disjoint circles. Each circle must bound a disk in $\Sigma_0 - G$ due to it being from a cellular embedding. If there is an innermost circle on A that bounds a disk in A , we can isotope A along a ball bounded by this disk and one in

$\Sigma_0 - G$ to remove the circle of intersection, where the ball exists by the irreducibility of $\Sigma \times I$. Hence, all the circles of intersection are essential in A . Each section of annulus is a cobordism from a nullhomotopic circle in $\Sigma_0 - G$, hence the two boundary circles of A are nullhomotopic as well. Thus, each section of annulus bounds a ball together with disks in $\Sigma \times \{0, \frac{1}{2}, 1\}$ not intersecting G , and the union of these form a ball that A bounds. \square

We give an algebraic proof of a weaker statement of this corollary in Remark 8.8.

By considering only representative surfaces, an alternative characterization of a virtual spatial graph is as a ribbon graph, some of whose vertices are 4-valent classical crossings. Equivalence is generated by gluing some number of disks into the boundary along disjoint arcs, performing one of the moves for regular isotopy or rigid vertex isotopy through these disks, and then deleting disks to destabilize the diagram to be a ribbon graph once again.

3. TWO INVARIANTS OF VIRTUAL GRAPHS

In this section we define two closely related polynomial invariants of virtual graphs. These invariants will later be considered in a more general context in Section 6, but for sake of a concrete definition we discuss them on their own first.

3.1. The flow polynomial. Since virtual graphs are abstract graphs equipped with additional data, abstract graph invariants such as the Tutte-Whitney polynomial — and specializations like the chromatic polynomial and the flow polynomial — are also invariants of virtual graphs up to move VI*. Recall the definition of the flow polynomial:

Definition 3.1. Let G be a graph and Q an indeterminate. The *flow polynomial* is given by the state sum formula

$$F_G(Q) = \sum_{T \subset E(G)} (-1)^{|T|} Q^{b_1(G-T)}.$$

Here $b_1(G-T) = \text{rank } H_1(G-T)$ is the first Betti number. Each “state” is a choice of which edges to exclude.

The combinatorial interpretation of the flow polynomial is that it counts the number of nowhere-zero Q -flows of a graph:

Definition 3.2. Let G be a graph and fix an arbitrary orientation of the edges of G , and let Q be a nonnegative integer. A *nowhere-zero Q -flow* of G is a coloring of its edges by nonzero elements of $\mathbb{Z}/Q\mathbb{Z}$ satisfying Kirchhoff’s Law: the signed sum (incoming sum minus outgoing sum) of the colorings at each vertex is zero. That is, a nowhere-zero Q -flow is a simplicial 1-cycle with coefficients in $\mathbb{Z}/Q\mathbb{Z}$, all of whose coefficients are nonzero.

A particular simplicial 1-cycle can be economically and freely determined by giving its coefficients at the edges outside a spanning tree of the graph, the number of which is counted by the first Betti number. The state sum can be viewed as an application of the inclusion-exclusion principle, where excluding a set T of edges is the same as forcing those edges to have zero for their coefficients, and the remaining degrees of freedom for such a simplicial 1-cycle is $b_1(G-T)$. Alternatively, one could instead check that both the state sum and combinatorial interpretations are invariant under the local relations in Definition 6.2.

One motivation for counting nowhere-zero Q -flows is that they are dual to Q -colorings: If G is a connected planar graph with dual graph G^* , then $F_G(Q) = Q^{-1} \chi_{G^*}(Q)$, where $\chi_{G^*}(Q)$ is the chromatic polynomial of the dual graph G^* .

3.2. The S -polynomial. We now define a graph polynomial closely related to the flow polynomial.

Definition 3.3. Let G be a virtual graph and Q an indeterminate. The S -polynomial is given by the state sum formula

$$S_G(Q) = \sum_{T \subset E(G)} (-1)^{|T|} Q^{b_1(G-T) - g(G-T)}.$$

The only difference from the flow polynomial is the $g(G-T)$ in the exponent, which incorporates topological information about the rotation system of the virtual graph. By construction, the S -polynomial is an invariant of virtual graphs. It is immediate from this state sum definition that $S_G(Q) = F_G(Q)$ in the case that G is a planar virtual graph, which is one way the S -polynomial is an extension of the flow polynomial.

The motivations for the S -polynomial are discussed in more detail in Section 6. Primarily, this invariant is the result of applying the functor in [10] to graphs on surfaces that might be non-planar. Secondarily, unlike the flow polynomial it is sensitive to the rotation system and can, for instance, distinguish the graphs in Figure 5. This gives a new extension of the Yamada polynomial in Section 8 to virtual spatial graphs.

The S -polynomial is a specialization of the Krushkal polynomial reformulated for cellular embeddings, the definition of which is given after the following. Given a surface graph $G \hookrightarrow \Sigma$, the *complementary genus* $g^\perp(G)$ (with Σ implicit) is the genus of the surface $\Sigma - \nu(G)$. If $G \hookrightarrow \Sigma$ is a cellular embedding, then recall that the dual graph $G^* \hookrightarrow \Sigma$ is from reversing the roles of vertices and faces, with the edges in G and G^* coming in dual pairs. If $T \subset E(G)$, then $g^\perp(G-T)$ is the genus of the induced subgraph of G^* whose edges are the edges dual to those in T .

Definition 3.4 ([16], section 4.2). The *Krushkal polynomial* when reformulated for a cellular embedding $G \hookrightarrow \Sigma$ is given by the state sum formula

$$P'_{G,\Sigma}(X, Y, A, B) = \sum_{T \subset E(G)} X^{b_0(G-T) - b_0(G)} Y^{b_1(G-T)} A^{2g(G-T)} B^{2g^\perp(G-T)}.$$

With G thought of as a virtual graph, define $P'_G = P'_{G,\Sigma}$.

Theorem 3.5. For G a virtual graph,

$$S_G(Q) = (-1)^{b_1(G)} P'_G(-1, -Q, Q^{-1/2}, 1).$$

Proof. Observe that

$$\begin{aligned} P'_G(-1, -Q, Q^{-1/2}, 1) &= \sum_{T \subset E(G)} (-1)^{b_0(G-T) - b_0(G)} (-Q)^{b_1(G-T)} Q^{-g(G-T)} \\ &= \sum_{T \subset E(G)} (-1)^{b_0(G-T) - b_1(G-T) - b_0(G)} Q^{b_1(G-T) - g(G-T)}. \end{aligned}$$

Using the Euler characteristics of $G - T$ and G ,

$$\begin{aligned} b_0(G-T) - b_1(G-T) &= |V(G-T)| - |E(G-T)| \\ &= |V(G)| - |E(G)| + |T| \\ &= b_0(G) - b_1(G) + |T|. \end{aligned}$$

Thus,

$$P'_G(-1, -Q, Q^{-1/2}, 1) = \sum_{T \subset E(G)} (-1)^{-b_1(G) + |T|} Q^{b_1(G-T) - g(G-T)}.$$

We can now pull out the overall factor of $(-1)^{b_1(G)}$ from the sum to give the desired formula. \square

4. CATEGORY OF VIRTUAL GRAPHS

In this section, we describe a category for virtual graphs up to edge subdivision. This is more generally a planar algebra, however a category serves well for our purposes.

Definition 4.1. The *virtual graph category* \mathbf{VG}^R over the ring R is a monoidal category whose objects are finite ordered sets $[n] = \{0, 1, \dots, n-1\}$ for $n \in \mathbb{N}$ and whose morphism sets $\mathbf{VG}^R([m], [n])$ are formal R -linear combinations of virtual graph diagrams, modulo edge subdivision, on oriented disks with $m+n$ marked 1-valent vertices along the boundary. Edges incident to the boundary are called *boundary edges*. Non-boundary edges are called *internal edges*. We imagine the $[m]$ points to be at the bottom of a diagram and the $[n]$ points to be at the top.

Composition $\mathbf{VG}^R([n], [\ell]) \times \mathbf{VG}^R([m], [n]) \rightarrow \mathbf{VG}^R([m], [\ell])$ is defined on individual virtual graphs by attaching the disks in an orientation-respecting way along a pair of arcs such that vertices $0, 1, \dots, n-1$ at the top of the second virtual graph are glued to the respective vertices $0, 1, \dots, n-1$ at the bottom of the first. The composition extends to linear combinations by linearity.

Monoidal composition is by the usual horizontal gluing along a pair of arcs disjoint from the marked points on the sides of the diagrams.

Ignoring edge subdivision and requiring there to be edges incident to the boundary vertices together allow for there to be an identity in $\mathbf{VG}^R([n], [n])$, namely the graph with n paths connecting vertex i at the bottom to vertex i at the top, for all $0 \leq i < n$. Virtual crossings satisfy move II*, so one may view a virtual crossing between two strands as a transposition, giving an embedding of the symmetric group ring $R[S_n]$ into $\mathbf{VG}^R([n], [n])$. This structure makes \mathbf{VG}^R a symmetric monoidal category. One could compare the case of a braided monoidal category, where the braiding is a crossing that is not necessarily an involution.

For now we will focus on virtual graphs, but there is a similar category \mathbf{VSG}^R of virtual spatial graphs, extending \mathbf{VG}^R with special marked 4-valent vertices called *classical crossings*.

The virtual graph category can be viewed as a planar diagram model for the category of graphs in surfaces with imposed symmetric monoidal structure.

Definition 4.2. The *surface graph category* over a ring R is a monoidal category whose objects are closed oriented 1-manifolds with finitely many marked points, and whose morphisms are formal R -linear combinations of oriented cobordisms between them with embedded surface graphs up to edge subdivision, intersecting the marked points transversely.

The full subcategory whose objects are 1-manifolds with exactly one marked point per connected component is a symmetric monoidal category, where an element of the symmetric group can be realized by a cobordism consisting of disjoint cylinders, each with an embedded path. However, this structure does not extend at the level of the embedded graphs to the case of 1-manifolds with more than one marked point. If we wish to represent elements of the symmetric group as paths on surfaces, then it suffices to consider the surfaces up to stable equivalence, keeping neighborhoods of the boundaries the same.

Definition 4.3. The *stable surface graph category* over a ring R is the surface graph category modulo stable equivalence of the cobordisms.

The isomorphism classes of objects in this category are determined by the number of marked points, and one could view them as stable equivalence classes of 0-manifolds embedded in 1-manifolds. By the same reasoning as Theorem 2.4 there is an equivalence of categories between the stable surface graph category and the virtual graph category.

5. THE BRAUER CATEGORY

Recall the definition of the Temperley-Lieb algebra TL_n^c , where $n \in \mathbb{N}$ and c is an indeterminate, sometimes chosen to be a specific complex number. TL_n^c is an algebra over $\mathbb{C}(c)$ spanned by

diagrams, oriented disks with properly embedded 1-manifolds (*strings*) up to isotopy rel boundary. The discs have the same $2n$ equally spaced boundary points, and the boundary points are partitioned into two sets of consecutive “top” and “bottom” points. (A manifold N is *properly* embedded in a manifold M if $N \cap \partial M = \partial N$ and this intersection is transverse.) A diagram with a closed loop bounding a disk (in the complement of the strings) is c times the same diagram without the loop.

Composition is given by gluing the bottom of the first diagram to the top of the second. There is a trace defined by gluing the top to the bottom; the resulting diagram is a collection of circles embedded in a sphere, so it evaluates to a scalar times the empty diagram. The Temperley-Lieb algebra is the endomorphism ring of a monoidal category, similar to that of Definition 4.2, but where the objects are instead arcs with marked points and where the morphisms are 1-manifolds embedded in disks cobounding these arcs.

Instead of disks we could consider diagrams drawn on surfaces. This is a version the surface graph category but with only embedded 1-manifolds, rather than graphs of arbitrary valence. Even after imposing the relation that closed loops bounding disks can be replaced by multiplication by c , diagrams without boundary points do not necessarily evaluate to a scalar because of lingering essential loops. For example, this is what leads to skein modules of dimension greater than one. If, however, we instead consider the stable surface graph category in Definition 4.3, then every loop bounds a disk in some representative surface graph of the stable equivalence class, and so they can be replaced with multiplication by c . This leads to a “virtual Temperley-Lieb category.”

Definition 5.1. The *Brauer category* Br^c is the subcategory of $\text{VG}^{\mathbb{C}(c)}$ generated by all virtual graphs that as surface graphs are properly embedded 1-manifolds, modulo multiplication by c being equivalent to inserting a closed loop. This definition is equivalent to modifying the Temperley-Lieb category to allow proper immersions of 1-manifolds rather than requiring proper embeddings.

The *Brauer algebra* $\text{Br}_n^c = \text{Br}^c([n], [n])$ is the endomorphism algebra for $[n]$, and it was introduced by Brauer in [5] for the Schur-Weyl duality of the orthogonal group. It is worth reviewing the map $\text{Br}^N([m], [n]) \rightarrow \text{Hom}_{SO(N)}(V^{\otimes m}, V^{\otimes n})$, where V is an inner product space, $N = \dim V$, and $m+n$ is even. A virtual graph diagram, drawn with $[m]$ at the bottom and $[n]$ at the top, is interpreted as an element of $(V^{\otimes m})^* \otimes V^n$ according to the following piece-by-piece correspondence, where $\{e_i\}_i$ is an orthonormal basis for V and $\{e^i\}_i$ the corresponding dual basis for V^* :

$$\begin{array}{ll} \square \mapsto \sum_i e^i \otimes e_i & \times \mapsto \sum_{i,j} e^i \otimes e^j \otimes e_j \otimes e_i \\ \cap \mapsto \sum_i e^i \otimes e^i & \vee \mapsto \sum_i e_i \otimes e_i \end{array}$$

Glued strands are contracted using the natural pairing between V and V^* . Notice that \cap is the inner product (evaluation map) and \vee is its “Casimir” (coevaluation map), and so they are related by the topological identity

$$(\cap \otimes \square) \circ (\square \otimes \vee) = \square = (\square \otimes \cap) \circ (\vee \otimes \square),$$

which in a less linear form can be represented as

$$\cap = \square = \vee.$$

The images of $\square^{\otimes a} \otimes \times^{\otimes b} \otimes \square^{\otimes c}$, with $a+2+b=n=m$, are induced by and generate the right action of the symmetric group S_n on the tensor power $V^{\otimes n}$. Loops are the composition $\cap \circ \vee$, and hence they evaluate to the dimension of V . This correspondence in fact determines an additive functor from Br^N to the full subcategory of $\text{Rep}(SO(N))$ (equivalently $\text{Rep}(\mathfrak{so}(N))$) generated by tensor powers of V .

The Brauer algebra is semisimple for generic values of c (see [23]), failing only at integers. The algebra Br_2^c will make a prominent appearance. It has the basis $\{\square\square, \square\cup\cap, \square\cap\cup\}$, and the primitive central idempotents for this algebra are

$$\begin{aligned} p_1 &= \frac{1}{c} \square\cup\cap \\ p_2 &= \frac{1}{2} \square\square - \frac{1}{2} \square\cap\cup \\ p_3 &= \frac{1}{2} \square\square - \frac{1}{c} \square\cup\cap + \frac{1}{2} \square\cap\cup. \end{aligned}$$

The element $p_2 + p_3 = \square\square - \frac{1}{c} \square\cup\cap$ is the Jones-Wenzl idempotent $P^{(2)}$ for the embedded Temperley-Lieb algebra.

6. CATEGORIES FOR INVARIANTS OF VIRTUAL GRAPHS

A large class of graph invariants, surface graph invariants, and ribbon graph invariants are determined by local relations, such as a form of contraction and deletion of edges. Examples include the Tutte-Whitney polynomial, its specializations the chromatic and flow polynomials, the Kruskal polynomial [16], the Bollobás-Riordan polynomial [4], the *S-polynomial* of Definition 3.3, and the $W_{\mathfrak{so}(N)}$ Penrose polynomial in Section 7. One way to interpret these invariants in a categorical context is to consider the quotient of a category like \mathbf{VG}^R by those local relations.

A sense in which local relations totally determine an algebraic invariant is that any graph with no external edges can be reduced to a scalar times an empty graph. This is equivalent to saying that $\text{End}(\mathbf{1})$ is isomorphic to the ring R of scalars for the category, where $\mathbf{1}$ is the monoidal unit. This perspective gives a motivation for stable equivalence: if there were no way to remove “far away” topology, $\text{End}([0])$ for quotients of the surface graph category could instead be like the situation for Kauffman bracket skein modules, which potentially are infinitely generated. Even in the case where every graph on a surface reduces to a scalar times the empty graph on the same surface, $\text{End}([0])$ would still be $R^{\mathbb{N}}$, with one copy of R for each homeomorphism class of surface.

In particular, graphical categories for which $\text{End}([0]) \cong R$ have a Markov trace. This trace is defined by connecting the top strands to the bottom strands, which removes all external edges, giving a diagram that evaluates to a scalar. Morphisms a such that $\text{tr}(ab) = 0$ for every b such that ab is an endomorphism correspond to local relations that preserve the invariant. Such an a is sometimes called a *negligible element*.

6.1. Edge contraction. In [7], Chmutov defines edge contraction for ribbon graphs by generalizing the fact for planar graphs that edge contraction corresponds to deleting the edge from the dual graph.

The *partial dual* of a virtual graph G at an edge e is described in [7] and [9], and the operation, which we will denote by $\delta_e G$, is illustrated in Figure 12. The operation is best understood as a manipulation of an *arrow presentation* for a ribbon graph, where the vertices of the ribbon graph are represented as closed disks with disjoint oriented labeled arcs on the boundaries, and the labels come in pairs to indicate how to glue in the edge disks.

The operation is an involution, and if e, e' are two edges in G , δ_e and $\delta_{e'}$ commute. The dual G^* of G is $\delta_{E(G)} G$, where $\delta_{E(G)}$ is the composition of all δ_e for $e \in E(G)$.

Definition 6.1. If G is a virtual graph and e is an edge in G , then G/e is defined to be $\delta_e G - e$, the virtual graph obtained by *contracting* the edge e .

This definition avoids the problem that the quotient of a surface by an embedded loop might not itself be a manifold. Instead, contracting a loop “splits” a vertex into two. This particular definition of contraction is not well-defined for abstract graphs.

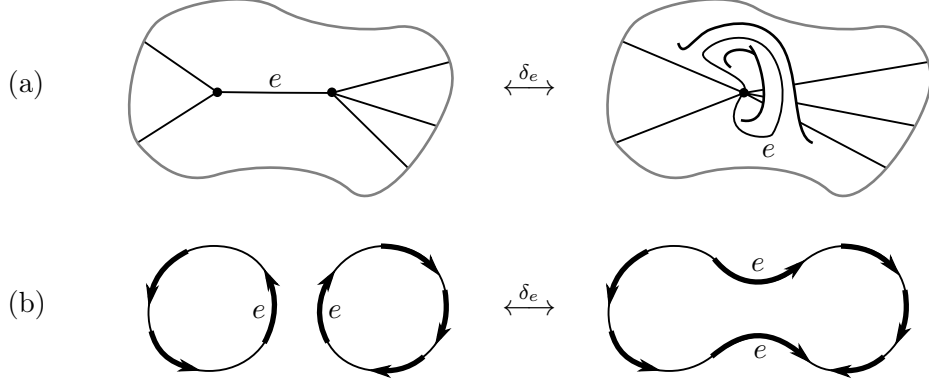


FIGURE 12. Two virtual graphs that are locally related by the partial dual operation at the edge e , (a) as a cellular embedding, and (b) as an arrow presentation of a ribbon graph.

6.2. The flow category. Before defining the category \mathbf{S}^Q for the S -polynomial, we motivate it with a more familiar example, the *flow category*. This category has been previously considered in, for instance, [1]. One way this category could be defined is as follows:

Definition 6.2. The *flow category* \mathbf{Flow}^Q is the quotient of $\mathbf{VG}^{\mathbb{C}(Q)}$ by the following local relations:

- (1) Contraction-deletion: For e an internal edge, if e is not a loop, $[G] = [G/e] - [G - e]$, and otherwise $[G] = (Q - 1)[G - e]$.
- (2) If $v \in V(G)$ is a degree-0 internal vertex, $[G] = [G - v]$.
- (3) If G has a degree-1 internal vertex, $[G] = 0$.
- (4) If G and G' are related by move VI* in Figure 11, $[G] = [G']$.

The *flow polynomial* $F_G(Q)$ is the image of G in $\mathbf{Flow}^Q([0], [0]) \cong \mathbb{C}(Q)$, with $F_\emptyset(Q) = 1$.

It is not hard to show by induction on the number of edges that this flow polynomial is equivalent to the state sum given in Definition 3.1. It is more natural to describe the flow category in terms of abstract graphs instead of virtual graphs, as in [1], but for sake of economical formalism we invoke move VI*.

6.3. The S -polynomial category. If G is a planar graph and $e \in E(G)$ is a loop, then $F_{G/e}(Q) = F_{G-e}(Q)$. This is because e must intersect G at exactly one point, so G/e is a disjoint union of two graphs G_1 and G_2 . The flow polynomial is known to be multiplicative under both disjoint union and wedge sum, and it is evident that $G/e \cong G_1 \amalg G_2$ and $G - e \cong G_1 \vee G_2$.

Thus, for planar graphs the contraction-deletion relations for the flow category can be unified as $[G] = Q^\epsilon[G/e] - [G - e]$, where ϵ is the difference between the Euler characteristics of G and G/e , which is 1 if e is a loop and 0 otherwise. One way to define the S -polynomial is to declare that we take this rule seriously for non-planar virtual graphs as well.

We will show that the S -polynomial is the invariant determined by the following axioms:

- (1) If G is the empty graph, $S_G(Q) = 1$.
- (2) If G is a single-vertex virtual graph with no edges, $S_G(Q) = 1$.
- (3) If G has a degree-1 vertex, $S_G(Q) = 0$.
- (4) If G_1, G_2 are virtual graphs, $S_{G_1 \amalg G_2}(Q) = S_{G_1}(Q)S_{G_2}(Q)$.
- (5) If e is an edge in a virtual graph G , $S_G(Q) = Q^\epsilon S_{G/e}(Q) - S_{G-e}(Q)$, where ϵ is the difference between the Euler characteristics of G and G/e .

Uniqueness of such a polynomial follows from the fact that the right-hand sides of each equation involve virtual graphs of less complexity, measured by the sum of the numbers of vertices and edges. While we could demonstrate existence by showing that the state sum in Definition 3.3 satisfies these

axioms, we will proceed by a more enlightening method: we construct a functor $\hat{\Phi} : \mathbf{VG}^{\mathbb{C}(Q)} \rightarrow \mathbf{Br}^{Q^{1/2}}$ that both satisfies the axioms and computes the state sum from $\mathbf{VG}^{\mathbb{C}(Q)}([0], [0])$.

Saying that the functor computes the polynomial means two things. The most obvious is that $\hat{\Phi}$ maps any virtual graph with no external edges to the S -polynomial of that graph. However, this will also be true for graphs with external edges, in the sense that if S^Q is the quotient of $\mathbf{VG}^{\mathbb{C}(Q)}$ by the local relations defining the S -polynomial, then $\hat{\Phi}$ factors through the quotient to give a trace-preserving functor $\Phi : S^Q \rightarrow \mathbf{Br}^{Q^{1/2}}$.

Consider $S_G^0(Q) \in \mathbb{C}[Q^{\pm 1/2}]$, related to the S -polynomial by the renormalization $S_G(Q) = Q^{(|E(G)|-|V(G)|)/2} S_G^0(Q)$. The axioms from above when renormalized appear as follows:

- (1) If G is the empty graph, $S_G^0(Q) = 1$.
- (2) If G is a single-vertex virtual graph with no edges, $S_G^0(Q) = Q^{1/2}$.
- (3) If G has a degree-1 vertex, $S_G^0(Q) = 0$.
- (4) If G_1, G_2 are virtual graphs, $S_{G_1 \amalg G_2}^0(Q) = S_{G_1}^0(Q) S_{G_2}^0(Q)$.
- (5) If e is an edge in a virtual graph G , $S_G^0(Q) = S_{G/e}^0(Q) - Q^{-1/2} S_{G-e}^0(Q)$.

The last of these axioms suggests a relationship to the second Jones-Wenzl idempotent $P^{(2)}$, which plays a role in the following definition for $\hat{\Phi}$.

Definition 6.3. The functor $\hat{\Phi} : \mathbf{VG}^{\mathbb{C}(Q)} \rightarrow \mathbf{Br}^{Q^{1/2}}$ is defined on objects by sending $[n]$ to $[2n]$, and it is defined on morphisms in the following piece-by-piece fashion:

- Edges are replaced by $Q^{1/2} P^{(2)} = Q^{1/2} \left(\begin{array}{c} \square \\ \square \end{array} \right) - Q^{-1/2} \left(\begin{array}{c} \square \\ \square \end{array} \right)$.
- Internal vertices are replaced according to

$$\begin{array}{ccc} \begin{array}{c} \diagup \\ \vdots \\ \diagdown \end{array} & \mapsto & Q^{-1/2} \begin{array}{c} \diagup \\ \vdots \\ \diagdown \end{array} \end{array}$$

- Boundary vertices at the bottom of a diagram are replaced by $Q^{-1/2} \left(\begin{array}{c} \square \\ \square \end{array} \right)$.
- Virtual crossings are replaced by $\begin{array}{c} \diagup \\ \diagdown \end{array}$.

These replacements along with the requirements that $\hat{\Phi}$ be monoidal and linear completely determine $\hat{\Phi}$. The normalization is the cause of the awkwardness in the difference between top and bottom boundary vertices — a functor for S^0 would not have these additional factors of $Q^{\pm 1/2}$.

Remark 6.4. There is a whole family of functors $\hat{\Phi}_k$ from $\mathbf{VG}^{\mathbb{C}(Q)}$ to $\mathbf{Br}^{Q^{1/2}}$ sending $[n]$ to $[kn]$ and edges to the Jones-Wenzl projector $P^{(k)}$, with k an even natural number.

Next we will show that this functor factors through another category, S^Q , to demonstrate the relationship to the S -polynomial.

Definition 6.5. The S -polynomial category S^Q is the quotient of $\mathbf{VG}^{\mathbb{C}(Q)}$ by the following local relations:

- (1) Contraction-deletion: For e an internal edge, $[G] = Q^\epsilon [G/e] - [G-e]$, where ϵ is the difference between the Euler characteristics of G and G/e .
- (2) If $v \in V(G)$ is a degree-0 internal vertex, $[G] = [G - v]$.
- (3) If G has a degree-1 internal vertex, $[G] = 0$.

A consequence of the functorial construction will be that $S^Q([0], [0]) \cong \mathbb{C}(Q)$, where at the moment one might only see that it is a quotient of $\mathbb{C}(Q)$. The image of a graph in this endomorphism ring will be its S -polynomial, because the relations for the category are equivalent to the axioms given for the invariant.

Theorem 6.6. $\hat{\Phi}$ factors through \mathbf{S}^Q to give a trace-preserving functor $\Phi : \mathbf{S}^Q \rightarrow \mathbf{Br}^{Q^{1/2}}$

Proof. For the following, let $G \in \mathbf{VG}^{\mathbb{C}(Q)}([m], [n])$.

If G has a degree-0 internal vertex, then the diagram for $\hat{\Phi}(G)$ contains $Q^{-1/2}$ times a loop, which evaluates to 1, and so $\hat{\Phi}(G) = \hat{\Phi}(G - v)$.

If G has a degree-1 internal vertex, then the diagram for $\hat{\Phi}(G)$ contains the composition $P^{(2)} \circ \boxed{V}$, where $P^{(2)}$ is from the edge incident to the vertex and \boxed{V} is from the vertex itself. But, $P^{(2)} \circ \boxed{V} = 0$, so $\hat{\Phi}(G) = 0$.

If $e \in E(G)$, one can show $\hat{\Phi}(G) = Q^\epsilon \hat{\Phi}(G/e) - \hat{\Phi}(G - e)$, with ϵ defined as it has been, by considering the two cases of e being a loop or non-loop, and by expanding e in the image as $Q^{1/2} \boxed{\parallel}$ and $-\boxed{V}$. The first of these expansions corresponds to $Q^\epsilon \hat{\Phi}(G/e)$, and the second to $-\hat{\Phi}(G - e)$.

Thus, $\hat{\Phi}$ factors through the morphism sets of \mathbf{S}^Q . It furthermore factors through the composition law and trace of \mathbf{S}^Q because only one of the two vertices being glued contributes a factor of $Q^{-1/2}$ in $\mathbf{Br}^{Q^{1/2}}$. \square

It is now established that the axioms give a well-defined polynomial invariant of virtual graphs. The correspondence to the state sum formulation will be proved in Theorem 6.10.

Remark 6.7. The definition of $\hat{\Phi}$ is the extension of the $\mathbf{TL}^{Q^{1/2}}$ construction for cubic planar graphs in [10] to virtual graphs. In that paper, Fendley and Krushkal find an infinite family of local relations for the flow polynomial (equivalently, the S -polynomial) of planar graphs by using the trace radical of the Temperley-Lieb algebra. This approach works because the trace radical is well-understood: it exists exactly when the loop parameter is a root of unity, and it is the tensor ideal generated by a Jones-Wenzl projector. The Jones-Wenzl projectors in turn have a straightforward combinatorial description.

There are similar, but more complicated results for projectors in the Brauer algebras [15, 18, 22]. We did not attempt to pull these back to the S -polynomial category, but instead we computed some local relations directly, as in Subsection 6.5.

Example 6.8. Let G_1 and G_2 respectively be the planar and toroidal theta graphs from Figure 5. It is a quick application of the axioms to calculate

$$S_{G_1}(Q) = (Q - 1)(Q - 2) \text{ and } S_{G_2}(Q) = -2(Q - 1).$$

Thus, the polynomial can distinguish virtual graphs with the same underlying graph. The two graphs in Figure 3 have S -polynomials $(Q - 1)^2$ and $Q - 1$, respectively. Another example is the complete bipartite graph $K_{3,3}$ as a virtual graph by connecting in \mathbb{R}^2 the points $(1, n)$ to all the points $(2, m)$, with $1 \leq m, n \leq 3$. $F_{K_{3,3}}(Q) = (Q - 1)(Q - 2)(Q^2 - 6Q + 10)$, whereas $S_{K_{3,3}}(Q) = (Q + 5)(Q - 1)(Q - 4)$. (The S -polynomials for $K_{3,3}$ with all possible rotation systems are $5(Q - 1)(Q - 4)$, $-(Q - 1)(Q - 4)(Q - 5)$, and $(Q + 5)(Q - 1)(Q - 4)$.)

Example 6.9. Alternatively, we could have computed the S -polynomial of the graphs of Figure 5 by the functor Φ . In Figure 13, $\boxed{\oplus}$ represents $\boxed{\parallel} - Q^{-1/2} \boxed{V}$, which in the expansion corresponds to the inclusion or exclusion an edge.

Theorem 6.10. Let G be a virtual graph. Then $\hat{\Phi}(G)$ is $S_G(Q)$ as defined by the state sum in Definition 3.3.

Proof. By viewing the two terms in $P^{(2)}$ as inclusion and exclusion of the edge, we see that the image of a virtual graph G is

$$Q^{(|E(G)| - |V(G)|)/2} \sum_{T \subset E(G)} (-1)^{|T|} Q^{(b_1(\partial(G - T)) - |T|)/2},$$

$$\begin{aligned}
\text{Diagram 1: } & \text{A circle with a horizontal chord.} \mapsto Q^{\frac{1}{2}} \text{Diagram 2} = Q^{\frac{1}{2}} \text{Diagram 3} - \text{Diagram 4} - \text{Diagram 5} + Q^{-\frac{1}{2}} \text{Diagram 6} \\
& - \text{Diagram 7} + Q^{-\frac{1}{2}} \text{Diagram 8} + Q^{-\frac{1}{2}} \text{Diagram 9} - Q^{-1} \text{Diagram 10} \\
& = Q^2 - Q - Q + 1 - Q + 1 + 1 - 1 \\
& = (Q - 1)(Q - 2) \\
\\
\text{Diagram 10: } & \text{A circle with two intersecting chords forming an '8' shape.} \mapsto Q^{\frac{1}{2}} \text{Diagram 11} = Q^{\frac{1}{2}} \text{Diagram 12} - \text{Diagram 13} - \text{Diagram 14} + Q^{-\frac{1}{2}} \text{Diagram 15} \\
& - \text{Diagram 16} + Q^{-\frac{1}{2}} \text{Diagram 17} + Q^{-\frac{1}{2}} \text{Diagram 18} - Q^{-1} \text{Diagram 19} \\
& = Q - Q - Q + 1 - Q + 1 + 1 - 1 \\
& = -2(Q - 1)
\end{aligned}$$

FIGURE 13. S -polynomials of theta graphs by the state sum from the $\hat{\Phi}$ functor.

where by $\partial(G - T)$ we mean the boundary components of a ribbon graph representative for $G - T$. Let $G - T \hookrightarrow \Sigma$ be a cellular embedding of the virtual graph. The induced map $H_1(G - T) \rightarrow H_1(\Sigma)$ is surjective, hence we obtain from the Mayer-Vietoris sequence the exact sequence

$$0 \rightarrow H_2(\Sigma) \rightarrow H_1(\partial(G - T)) \rightarrow H_1(G - T) \oplus H_1(\Sigma - (G - T)) \rightarrow H_1(\Sigma) \rightarrow 0,$$

where $H_1(\Sigma - (G - T)) = 0$. With $b_i(X) := \text{rank } H_i(X)$ being the i th Betti number of a space X , the Euler characteristic of this exact sequence gives the equation

$$0 = b_2(\Sigma) - b_1(\partial(G - T)) + b_1(G - T) - b_1(\Sigma).$$

Hence we may obtain the following expression for the Euler characteristic of Σ :

$$\begin{aligned}
\chi(\Sigma) &= b_2(\Sigma) - b_1(\Sigma) + b_0(\Sigma) \\
&= b_1(\partial(G - T)) - b_1(G - T) + b_0(\Sigma) \\
&= b_1(\partial(G - T)) - b_1(G - T) + b_0(G - T) \\
&= b_1(\partial(G - T)) - |E(G - T)| + |V(G - T)|,
\end{aligned}$$

using $b_0(G - T) - b_1(G - T) = |V(G - T)| - |E(G - T)|$.

Since $|E(G - T)| = |E(G)| - |T|$, we have $b_1(\partial(G - T)) - |T| = \chi(\Sigma) + |E(G)| - |V(G)| - 2|T|$, and so the state sum is equivalently

$$\begin{aligned}
S_G(Q) &= \sum_{T \subset E(G)} (-1)^{|T|} Q^{|E(G)| - |V(G)| + \chi(\Sigma)/2 - |T|} \\
&= \sum_{T \subset E(G)} (-1)^{|T|} Q^{b_1(G - T) - g(G - T)},
\end{aligned}$$

which matches Definition 3.3. □

Lemma 6.11. $S^Q([m], [n])$ has a basis in one-to-one correspondence with fixed-point-free permutations of the $(m + n)$ boundary half-edges. In particular, if $\sigma \in S_{m+n}$, each cycle in the cycle decomposition of σ is an interior vertex, and the cycle is the rotation system for the vertex.

Proof. By contraction-deletion, we may assume a particular element has no interior edges, and we may remove isolated interior vertices, hence the described set spans $S^Q([m], [n])$ since a fixed point would correspond to a degree-1 interior vertex. For independence, consider the image under Φ . In the expansion of an element corresponding to a permutation, the term corresponding to sending every edge to  can be used to recover the permutation. This term can be identified by the fact that the only strands are between even boundary vertices or between odd boundary vertices, where boundary vertices in $\text{Br}^{Q^{1/2}}([2m], [2n])$ are *even* or *odd* depending on the parity of its numeric label. These terms are linearly independent in $\text{Br}^{Q^{1/2}}([2m], [2n])$, hence the described set is independent. \square

Theorem 6.12. *Let G be a virtual graph. G has a bridge edge if and only if $S_G(Q) = 0$. If G has no bridge edge, $S_G(Q)$ is monic and $\deg S_G(Q) = b_1(G) - g(G)$.*

Proof. If G has a bridge edge, then G can be represented as the composition of an element in $\text{VG}^Q([0], [1])$ and an element in $\text{VG}^Q([1], [0])$. However, $S^Q([0], [1])$ and $S^Q([1], [0])$ are both zero-dimensional, hence $S_G(Q) = 0$. Suppose now that G has no bridge edges.

We will show that the exponent $b_1(G - T) - g(G - T)$ in the state sum of Definition 3.3 is maximized exactly when $T = \emptyset$, where $T \subset E(G)$. Since $2(b_1(G - T) - g(G - T)) = |E(G)| - |V(G)| + b_1(\partial(G - T)) - |T|$, we will maximize $\Psi(T) := b_1(\partial(G - T)) - |T|$ in particular. Consider an arbitrary subset $T \subset E(G)$ and an edge $e \in E(G) - T$. Let $T' = T \cup \{e\}$. When adding the edge e to T , $b_1(\partial(G - T))$ changes depending on the structure of the boundary circles near e . Let a and b denote the boundary circles of $G - T$ on either side of e , oriented so that at e they have the same local orientation, and we proceed by cases.

Case I: a and b are the same curve, and they have opposite orientation. Then $b_1(\partial(G - T')) = b_1(\partial(G - T)) + 1$, and so $\Psi(T') = \Psi(T)$.

Case II: a and b are the same curve, and they have the same orientation. Then G would have to be embedded in an unorientable surface. (While this cannot happen, $\Psi(T') = \Psi(T) - 1$.)

Case III: a and b are different curves. Then $b_1(\partial(G - T')) = b_1(\partial(G - T)) - 1$, hence $\Psi(T') = \Psi(T) - 2$.

Thus, $T = \emptyset$ is maximal with respect to Ψ . If there were an edge e such that $b_1(\partial(G - e)) - 1 = b_1(\partial G)$ (that is, Case I), then e would be a bridge edge. Since we assumed G has no bridge edges, $T = \emptyset$ is the only term contributing to the maximal possible degree, and so the other terms of the state sum do not cancel it out. Therefore, $S_G(Q)$ is monic with degree $b_1(G) - g(G)$. \square

Remark 6.13. There is also a functor $\text{VG}^{\mathbb{C}(Q)} \rightarrow \text{Br}^{-Q^{1/2}}$ to calculate the S -polynomial, with the edges being replaced instead by some normalization of $P^{(2)} = \boxed{\text{II}} + Q^{-1/2} \boxed{\text{V}} \boxed{\text{O}}$. An extension of the S -polynomial to graphs embedded in unorientable surfaces could be done by replacing half twists with  in either expansion, and yielding distinct invariants.

6.4. Connect sums and the S -polynomial.

Definition 6.14. Let G_1 and G_2 be virtual graphs, each with a distinguished oriented edge. Decompose the graphs as $G_1 = G'_1 \circ \boxed{\text{V}}$ and $G_2 = \boxed{\text{O}} \circ G'_2$, where  and  are the distinguished edges, co-oriented left-to-right. The *edge connect sum* of G_1 and G_2 at their respective edges is the virtual graph $G'_1 \circ G'_2$, written $G_1 \#_2 G_2$.

Lemma 6.15. *If G_1 and G_2 are virtual graphs, $(Q - 1)S_{G_1 \#_2 G_2}(Q) = S_{G_1}(Q)S_{G_2}(Q)$, no matter the choice or orientation of the distinguished edges.*

Proof. $S^Q([1], [1])$ is one-dimensional and its trace is non-degenerate. Hence, if G is a virtual graph that is $\text{tr } G'$ for $G' \in \text{VG}^Q([1], [1])$, the image of G' in $\text{Sc}^Q([1], [1])$ is $\frac{S_G(Q)}{Q-1} \boxed{\text{I}}$. By duality, a similar result applies for $S^Q([2], [0])$ and $S^Q([0], [2])$.

Decompose G_1 and G_2 as G'_1 and G'_2 as in Definition 6.14. Their images in $S^Q([2], [0])$ and $S^Q([0], [2])$ are $\frac{S_{G_1}(Q)}{Q-1}$  and $\frac{S_{G_2}(Q)}{Q-1}$ , respectively. The conclusion follows from  \circ  $= Q-1$. \square

Definition 6.16. Let G_1 and G_2 be virtual graphs each with a distinguished degree-3 vertex and incident half edge. Decompose G_1 as $G'_1 \circ$  and G_2 as  $\circ G'_2$ with the distinguished half edges left-most in  and . The composition $G'_1 \circ G'_2$ is the (*trivalent*) *vertex connect sum* $G_1 \#_3 G_2$ for the distinguished vertices.

For a virtual graph G with vertex v , let $\sigma_v G$ be G except that v is given the opposite rotation. The *twisted (trivalent) vertex connect sum* is $G_1 \#_3 \sigma_v G_2$, for $v \in V(G_2)$. For both vertex connect sums, the order of G_1 and G_2 does not matter.

Lemma 6.17. Let G_1 and G_2 be virtual graphs with distinguished degree-3 vertices v_1 and v_2 , respectively. Then

$$(Q-1)(Q-2)S_{G_1 \#_3 G_2}(Q) - 2(Q-1)S_{G_1 \#_3 \sigma_{v_2} G_2}(Q) = S_{G_1}(Q)S_{\sigma_{v_2} G_2}(Q) + S_{\sigma_{v_1} G_1}(Q)S_{G_2}(Q).$$

Proof. The space $S^Q([3], [0])$ has the basis   and $S^Q([0], [3])$ the basis  . The argument is similar to the one in Lemma 6.15, but each graph is represented as a composition with a trivalent vertex. By writing G'_1 and G'_2 in terms of the respective bases, we can expand both sides of the required equation. The coefficients are the S -polynomials the two theta graphs. \square

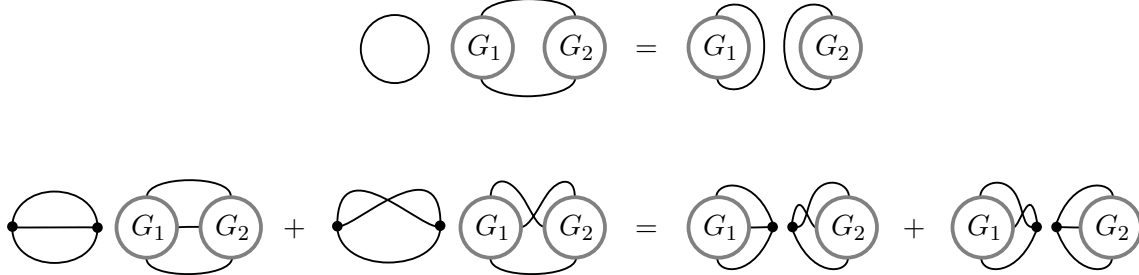


FIGURE 14. Graphical representations of the edge and vertex connect sum relations.

6.5. Local relations for the S -polynomial. The S -polynomial has additional local relations at certain evaluations of Q . The idea is that there is a pairing between $S^Q([n], [0])$ and $S^Q([0], [n])$ by composition, and when this pairing is degenerate, elements in the radical of the pairing (that is, the kernel of the pairing as a map $S^Q([n], [0]) \rightarrow S^Q([0], [n])^*$) give local linear relations. This is a slight generalization of the use of negligible elements.

The space $S^Q([3], [0])$ has the basis  , and the Gramian matrix of the pairing with respect to this basis is

$$\begin{pmatrix} (Q-1)(Q-2) & -2(Q-1) \\ -2(Q-1) & (Q-1)(Q-2) \end{pmatrix},$$

which is singular when $Q = 0, 1, 4$. For $Q = 0$, the radical is spanned by  $-$ , implying the local relation $S_{\#_3 \circ G}(0) = S_{\#_3 \circ G}(0)$, where $G \in VG^Q([0], [3])$. Similarly, for $Q = 4$, the radical is spanned by  $+$ , implying $S_{\#_3 \circ G}(4) = -S_{\#_3 \circ G}(4)$. This is depicted in the form of a relation in a planar algebra in Figure 15. The $Q = 1$ case is uninteresting, and it is a direct consequence of the state sum that $S_G(1) = 0$ for all G .

Lemma 6.18. If G is a virtual graph, $S_G(0) = F_G(0)$.

FIGURE 15. The local relation at $Q = 4$ for the S -polynomial. This is a relation on morphisms in the category S^4 .

Proof. The S -polynomial at $Q = 0$ has the additional local relation $\square \text{ (a)} = \square \text{ (b)}$. A consequence of the contraction-deletion relation is that then the polynomial is invariant under move VI*, and so the S -polynomial has the same axioms as the flow polynomial at this evaluation. \square

Lemma 6.19. *Let G be a cubic virtual graph whose underlying graph is planar, and let n be the number of vertex flips necessary to achieve planarity. Then $(-1)^n S_4(G) = F_4(G)$, counting the number of edge 3-colorings.*

Proof. Let G be a cubic virtual graph whose underlying graph is planar. By repeatedly using the local relation at $Q = 4$, $S_4(G) = (-1)^n S_4(G')$, where G' is a planar virtual graph with the same underlying graph, and where n is the number of vertex flips used to get there. The result then follows from the equivalence of the two polynomials for planar graphs. \square

There are other similar linear local relations at specific evaluations of Q . The following conjecture is from computational evidence for $S^Q([n], [0])$ with $n = 2, 3, 4, 5$.

Conjecture 6.20. *$S_Q(G)$ has additional local relations at $Q = n^2$ with n an integer. In particular, the trace form is degenerate for $S^Q([n], [0])$ exactly at $Q = 1^2, 2^2, \dots, (n-1)^2$, and additionally at $Q = 0$ when $n \geq 3$.*

There is also a representation-theoretic motivation for this conjecture. In [10], Fendley and Krushkal find local relations for planar graphs with n boundary strands at the values

$$Q = 4 \cos^2 \left(\frac{\pi k}{2n+1} \right),$$

where $k < 2n$. For $k = 1$ these are the Beraha numbers, which are conjectured to be accumulation points of the zeros of chromatic polynomials of planar triangulations.

Fendley and Krushkal find these relations as a consequence of the representation theory of $\mathcal{U}_q(\mathfrak{sl}_2)$, which can be described graphically by Temperley-Lieb diagrams. When q is a root of unity, the category of representations is not semisimple, certain representations that are well-defined for generic q fail to exist and there is a nontrivial trace radical, generated by a Jones-Wenzl idempotent. Because the loop value $c = Q^{1/2}$ of the Temperley-Lieb category is interpreted as the *quantum integer* $[2]_q = q + q^{-1}$, $Q = [2]_q^2 = (e^{\pi i k/N} + e^{-\pi i k/N})^2$ takes the above form.

As previously discussed, passing to nonplanar graphs requires the use of the Brauer category instead of the Temperley-Lieb category. In this case, the special loop values are no longer $q + q^{-1}$ for q a root of unity, but integers, as shown by Wenzl [23], who computed that the Brauer algebras fail to be semisimple exactly when the loop value is integral. Because Q corresponds to the square of the loop value under the functor Φ , local relations for the S -polynomial should occur at squares of integers.

Finally, since there seem to be some connections between the flow polynomial and the S -polynomial, we mention that Jacobsen and Salas [12] make a similar conjecture based on computational evidence for the flow and chromatic polynomials for certain families of nonplanar graphs, that the analogue for the Beraha numbers for nonplanar graphs are simply the nonnegative integers.

6.6. Virtual chromatic polynomial. We consider a virtual graph version of the chromatic polynomial, defined by analogy to the axioms for the S -polynomial from the flow polynomial. For G a virtual graph, the Laurent polynomial $\lambda_G(t)$ is determined by the following:

- If G is a collection of n isolated vertices, $\lambda_G(t) = t^n$.
- If $e \in E(G)$ is a non-loop edge, $\lambda_G(t) = \lambda_{G-e}(t) - \lambda_{G/e}(t)$.
- If $e \in E(G)$ is a loop edge, $\lambda_G(t) = \lambda_{G-e}(t) - t^{-1}\lambda_{G/e}(t)$.

Lemma 6.21. *Letting G be a virtual graph, then $\lambda_G(Q) = Q^{1-g(G)}S_{G^*}(Q)$. Equivalently, $S_G(Q) = Q^{g(G)-1}\lambda_{G^*}(Q)$. Therefore λ_G is well-defined, and for planar graphs λ_G is the chromatic polynomial.*

Proof. Let $\lambda_G^0(Q) = S_{G^*}^0(Q)$. For $e \in E(G)$ and $F = E(G) - e$,

$$\begin{aligned} \lambda_G^0(Q) &= S_{\delta_{E(G)}G}^0(Q) = S_{\delta_F G - e}^0(Q) - Q^{-1/2}S_{\delta_e \delta_F G - e}^0(Q) \\ &= S_{\delta_F(G-e)}^0(Q) - Q^{1/2}S_{\delta_F(\delta_e G - e)}^0(Q) \\ &= \lambda_{G-e}^0(Q) - Q^{-1/2}\lambda_{G/e}^0(Q). \end{aligned}$$

We will show $\lambda_G(Q) = Q^{|V(G)|/2}\lambda_G^0(Q)$.

If G is a collection of isolated vertices, $Q^{|V(G)|/2}\lambda_G^0(Q) = S_G^0(Q) = Q^{|V(G)|/2}S_G^0(Q) = Q^{|V(G)|}$. If $e \in E(G)$ is a loop edge or a non-loop edge, then one can check that $Q^{|V(G)|/2}\lambda_G^0(Q)$ has the same deletion-contraction relation as $\lambda_G(Q)$.

Then, $\lambda_G(Q) = Q^{|V(G)|/2}S_{G^*}^0(Q) = Q^{(|V(G)|-|E(G)|+|V(G^*)|)/2}S_{G^*}(Q)$, and the result follows from $|V(G)| - |E(G)| + |V(G^*)| = 2 - 2g(G)$. \square

7. PENROSE POLYNOMIALS

In [20], Penrose introduced tensor diagrams and calculated invariants of virtual graphs from interpreting each vertex as a tensor with edges representing contraction via some nondegenerate form, and he demonstrated the correspondence between the $\mathfrak{so}(3)$, $\mathfrak{sl}(2)$, and “ $\mathfrak{so}(-2)$ ” invariants, where the “dimension” is $\sum_i \langle e_i, e^i \rangle$ when $\{e_i\}_i$ and $\{e^i\}_i$ are bases dual with respect to the form. The more general case is summarized in [3], which associates to a metric Lie algebra \mathfrak{g} a scalar invariant $W_{\mathfrak{g}}(G)$ of a virtual graph G , all of whose vertices are degree 2 or 3, by replacing each degree-2 vertex with $\langle -, - \rangle$, each degree-3 vertex with the invariant 3-form $\langle -, [-, -] \rangle$, and each edge the Casimir element (in other words, this is an invariant from coloring the graph by the adjoint representation of \mathfrak{g} , where the orientation of the edges is irrelevant since the metric gives $\mathfrak{g} \cong \mathfrak{g}^*$). The invariants $W_{\mathfrak{sl}(N)}(G)$, $W_{\mathfrak{so}(N)}(G)$, and $W_{\mathfrak{sp}(2N)}(G)$ are polynomials in N , and these are called the *Penrose polynomials*. By rescaling the 2- and 3-forms, the Penrose polynomials might vary by a normalization factor of $a^{|V(G)|}b^{|E(G)|}$ with a, b functions of N independent of the graph.

The $W_{\mathfrak{so}(N)}$ polynomial was extended in [2] for planar graphs with vertices of arbitrary degree, and again in [9] for surface graphs. An algebra of connected cubic virtual graphs modulo the IHX relation is considered in [8], and, with multiplication being edge connect sum, the map to the Penrose polynomials is a homomorphism.

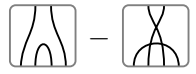
7.1. Via the Brauer category. In this section, we reiterate [20] and [3] for $W_{\mathfrak{so}(N)}$ and $W_{\mathfrak{sl}(N)}$ in terms of the Brauer category and virtual graphs. Let k be a field, and consider the vector space k^N with the standard inner product, giving an isomorphism $k^N \cong (k^N)^*$ and a correspondence between $\mathfrak{gl}(N) = \text{End}_k(k^N)$ and $k^N \otimes k^N$. The trace operator $\text{tr} : \mathfrak{gl}(N) \rightarrow k$ under this correspondence is $A \mapsto \text{[} \cap \text{]} \circ A$, and matrix multiplication is $A \otimes B \mapsto (\text{[} \cap \text{]} \otimes \text{[} \cap \text{]} \otimes \text{[} \cap \text{]}) \circ (A \otimes B)$. The Killing form on $\mathfrak{gl}(N)$ is a scale multiple of the trace form $A \otimes B \mapsto \text{tr}(AB)$, and thus is a scale multiple of

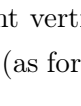
$$A \otimes B \mapsto \text{[} \cap \text{]} \circ (A \otimes B).$$

The vertical reflection  is the Casimir, and  \circ  $= N^2 = \dim(\mathfrak{gl}(N))$. The anti-involution $A \mapsto A^T$ is composition with , and since $BA = (A^T B^T)^T$ we have the following representation for the Lie bracket:

$$[A, B] = \left(\begin{array}{c} \text{---} \\ | \\ \text{---} \end{array} - \begin{array}{c} \text{---} \\ | \\ \text{---} \end{array} \right) \circ (A \otimes B).$$

The algebra Br_2^N contains projectors onto $\mathfrak{so}(N)$ and $\mathfrak{sl}(N)$. The element $\frac{1}{2} \begin{array}{c} \text{---} \\ | \\ \text{---} \end{array} - \frac{1}{2} \begin{array}{c} \text{---} \\ | \\ \text{---} \end{array}$ is the antisymmetrizer, and thus projects onto $\mathfrak{so}(N)$. The element  :=  $- \frac{1}{N} \begin{array}{c} \text{---} \\ | \\ \text{---} \end{array}$ eliminates the trace of a matrix, since composition with it is equivalent to $A \mapsto A - \frac{\text{tr} A}{N} \text{id}_N$, and thus projects onto $\mathfrak{sl}(N)$.

The Penrose polynomials, then, can be calculated by replacing each (trivalent) vertex with  and each edge with the respective projector, due to their relatively simple Killing forms. Virtual crossings are replaced with . We are being cavalier with “top” and “bottom” with the diagrams because self-duality affords us this liberty.

There are some shortcuts one may take to calculate these Penrose polynomials. For $W_{\mathfrak{so}(N)}$, since  negates the antisymmetrizer,  \circ  \circ ( \otimes = - \begin{array}{c} \text{---} \\ | \\ \text{---} \end{array}. Hence, up to normalization, we may replace trivalent vertices with  and edges with  $- \begin{array}{c} \text{---} \\ | \\ \text{---} \end{array}$. We can extend this to arbitrary virtual graphs (as for surface graphs in [9]) using the following replacement:

$$\begin{array}{c} \text{---} \\ | \\ \text{---} \end{array} \mapsto \begin{array}{c} \text{---} \\ | \\ \text{---} \end{array}$$

while still replacing edges with  $- \begin{array}{c} \text{---} \\ | \\ \text{---} \end{array}$. Note that isolated vertices contribute a factor of N .

For $W_{\mathfrak{sl}(N)}$, we may replace edges that are incident to trivalent vertices with  rather than  because $\text{tr}[-, -] = 0$ and because of rotational symmetry. Loops evaluate to $N^2 - 1$.

7.2. Relations for $W_{\mathfrak{so}(N)}$. In this section, we describe the “contraction-deletion” relations for $W_{\mathfrak{so}(N)}$ present in [9], but in terms of virtual graphs. In that paper, Ellis-Monaghan and Moffat use the *twisted dual* operation for graphs on unoriented surfaces, yet we have only been considering oriented surfaces. Nevertheless, we will derive a contraction-deletion relation directly from the Brauer algebra replacement rules, but we will also show how to augment our virtual graph notation to accommodate the description of contraction-deletion with the twisted dual.

Let  :=  $- \begin{array}{c} \text{---} \\ | \\ \text{---} \end{array}$. In general, a solid bar across n strands in Penrose notation is $\sum_{\sigma \in S_n} (-1)^\sigma \sigma_*$.

Lemma 7.1. *For $W_{\mathfrak{so}(N)}$, the following relation holds for a non-loop edge:*

$$\begin{array}{c} \text{---} \\ | \\ \text{---} \end{array} \text{---} \begin{array}{c} \text{---} \\ | \\ \text{---} \end{array} = \begin{array}{c} \text{---} \\ | \\ \text{---} \end{array} \text{---} \begin{array}{c} \text{---} \\ | \\ \text{---} \end{array} - (-1)^m \begin{array}{c} \text{---} \\ | \\ \text{---} \end{array}$$

where m is the number of half edges incident to the right vertex, not including the edge to be contracted. For a loop edge,

$$\text{Diagram} = \text{Diagram} - (-1)^m \text{Diagram}$$

where m is the number of edges between the two half edges of the loop on the right side.

Proof.

$$\begin{aligned} \text{Diagram} &= \text{Diagram} - \text{Diagram} \\ &= \text{Diagram} - (-1)^m \text{Diagram} \end{aligned}$$

where the second equality is from flipping the right-hand cluster over by introducing $m+1$ $\boxed{\times}$'s, then using the fact that $\boxed{\times} \circ \boxed{-} = -\boxed{-}$ for each of the m $\boxed{-}$'s. The proof for loop edges is similar, but be aware that when $m=0$ contraction introduces an isolated vertex. \square

Corollary 7.2. $W_{\mathfrak{so}(N)}(G) - W_{\mathfrak{so}(N)}(G/e) = W_{\mathfrak{so}(N)}(\delta_e G) - W_{\mathfrak{so}(N)}(\delta_e G/e)$. That is,

$$\text{Diagram} - \text{Diagram} = \text{Diagram} - \text{Diagram}.$$

As temporary notation, for an edge $e \in E(G)$ with a distinguished half edge, let $G \curlywedge e$ denote the second term for each relation, where the distinguished half edge is the side where the rotation is reversed, which for a loop we mean the half edges clockwise from it. The following relations give a recursive method to calculate $W_{\mathfrak{so}(N)}(G)$.

- (1) If $v \in V(G)$ is an isolated vertex, $W_{\mathfrak{so}(N)}(G) = NW_{\mathfrak{so}(N)}(G)$.
- (2) If $v \in V(G)$ is a vertex of degree 1, $W_{\mathfrak{so}(N)}(G) = 0$.
- (3) For any edge $e \in E(G)$, $W_{\mathfrak{so}(N)}(G) = W_{\mathfrak{so}(N)}(G/e) - (-1)^m W_{\mathfrak{so}(N)}(G \curlywedge e)$, where $m+1$ is the number incident half edges from the distinguished end of e .
- (4) $W_{\mathfrak{so}(N)}(G_1 \amalg G_2) = W_{\mathfrak{so}(N)}(G_1)W_{\mathfrak{so}(N)}(G_2)$

Other rules include:

- Subdividing an edge multiplies $W_{\mathfrak{so}(N)}$ by 2. (This is due to the normalization.)
- If e is a loop whose half edges are sequentially incident, then

$$W_{\mathfrak{so}(N)}(G) = (N-1)W_{\mathfrak{so}(N)}(G - e).$$

- Flipping a degree- m vertex over (the virtual version of move V) multiplies by $(-1)^m$.
- If v is a degree-3 vertex with a loop, $W_{\mathfrak{so}(N)}(G) = 0$.

- The IHX relation from ad-invariance of the Lie bracket: $\text{Diagram} = \text{Diagram} + \text{Diagram}$.

Now we will extend the graphs under consideration with special 2-valent vertices representing half twists, subject to the relations in Figure 16, where the twists are represented as open circles. We do not consider half twists to subdivide edges, and instead we imagine the twists to lie along an edge. In the evaluation of $W_{\mathfrak{so}(N)}$, half twists are replaced with the anti-involution $\boxed{\times}$. For an edge e in G , let $\tau_e G$ denote G with an additional twist along e . When there are no twists along e , which can always be arranged when e is not a loop, then $\delta_e G$ is defined as it was for virtual graphs

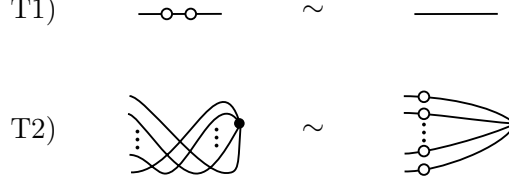
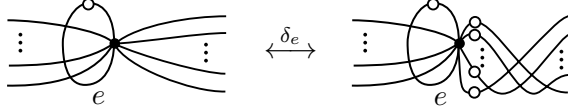


FIGURE 16. Moves for half twists.

FIGURE 17. The partial duality operation for a loop e with a single twist along it.

without twists in Figure 12. When e is a loop with a twist, then by similarly considering a dual graph for a cellular embedding (in an unoriented surface), or by considering the arrow presentation, partial duality is given by the more complicated transformation in Figure 17. The effect of twisting is that $W_{\mathfrak{so}(N)}(\tau_e G) = -W_{\mathfrak{so}(N)}(G)$. Hence, Lemma 7.1 can be restated in a form closer to that in [9] by saying that for any edge e in G ,

$$W_{\mathfrak{so}(N)}(G) = W_{\mathfrak{so}(N)}(\delta_e G - e) - W_{\mathfrak{so}(N)}(\delta_e \tau_e G - e),$$

or, using $G/e = \delta_e G - e$, that $W_{\mathfrak{so}(N)}(G) = W_{\mathfrak{so}(N)}(G/e) - W_{\mathfrak{so}(N)}(\tau_e G/e)$.

By extending $W_{\mathfrak{sl}(N)}$ to accommodate half twists, using the same correspondence that a half twist is replaced with the anti-involution $\bigcirc\!\!\!\times$, we obtain the following relationship:

Lemma 7.3. *With a suitable normalization for the Penrose polynomials,*

$$W_{\mathfrak{so}(N)}(G) = \sum_{S \subset E(G)} (-1)^{|S|} W_{\mathfrak{sl}(N)}(\tau_S G),$$

where τ_S is the composition of all τ_s for $s \in S$.

Proof. This follows from the analysis of the primitive central idempotents for Br_2^N . In particular,

$$\left(\frac{1}{2} \big| \big| \big| - \frac{1}{2} \bigcirc\!\!\!\times \right) \circ \left(\big| \big| \big| - \frac{1}{N} \big| \big| \big| \right) = \frac{1}{2} \big| \big| \big| - \frac{1}{2} \bigcirc\!\!\!\times.$$

□

7.3. Relations for $W_{\mathfrak{sl}(N)}$. For v a vertex in a virtual graph G , let $\sigma_v G$ be the graph obtained from reversing the rotation system at v .

Lemma 7.4. *With a suitable normalization, we can give $W_{\mathfrak{sl}(N)}$ in terms of the S -polynomial for a cubic virtual graph G as*

$$W_{\mathfrak{sl}(N)}(G) := \sum_{W \subset V(G)} (-1)^{|W|} S_{\sigma_W(G)}(N^2),$$

where σ_W is the composition of all σ_v for $v \in W$.

Proof. This is a state sum from expanding the vertices as $\big| \big| \big|$ and $-\bigcirc\!\!\!\times$. □

Let $g_{\min}(G)$ be the minimal genus over all rotation systems of a cubic virtual graph G :

$$g_{\min}(G) = \min_{W \subset V(G)} g(\sigma_W(G)).$$

It follows from Theorem 6.12 that $\deg W_{\mathfrak{sl}(N)}(G) \leq 2b_1(G) - 2g_{\min}(G)$.

Lemma 7.5 (Bar-Natan [3]). *If G is a cubic virtual graph with no bridge edges, the underlying graph of G is planar if and only if $\deg W_{\mathfrak{sl}(N)}(G) = 2b_1(G)$.*

Proof. In the expansion, the only $S_{\sigma_W(G)}(N^2)$ terms with maximal degree are the ones for which $\sigma_W(G)$ is a planar. By a theorem of Whitney, planar embeddings of cubic graphs are related by moves that flip over one subgraph in an edge-connect-sum decomposition, and any such subgraph has an even number of vertices. Therefore, the terms corresponding to planar embeddings do not cancel out in the sum. \square

There is no equality in general because, for example, $W_{\mathfrak{sl}(N)}(K_{3,3}) = 0$.

Lemma 7.6. *If G is a cubic virtual graph, $W_{\mathfrak{sl}(2)}(G) = 2^{|V(G)|} S_G(4)$.*

Proof. In the vertex expansion state sum, we have $S_{\sigma_W(G)}(4) = (-1)^{|W|} S_G(4)$, so the coefficient cancels. \square

Lemma 7.7 (Penrose [20]). *For a cubic virtual graph G , $W_{\mathfrak{so}(3)}(G)$ and $W_{\mathfrak{so}(-2)}(G)$ are equal up to a suitable normalization.*

Proof. We provide a short algebraic proof. From Lemma 7.4, it is clear that $W_{\mathfrak{sl}(-2)}(G) = W_{\mathfrak{sl}(2)}(G)$. The algebra Br_2^{-2} has  +  +  in its trace radical, so in the quotient there is the relation  = $-\square - \bigcirc$, which Penrose calls the *binor identity*. Since  \circ  = 0, we have the relation $W_{\mathfrak{sl}(-2)}(\tau_v G) = -W_{\mathfrak{sl}(-2)}(G)$, hence Lemma 7.3 implies $W_{\mathfrak{so}(-2)} = 2^{|E(G)|} W_{\mathfrak{sl}(-2)}(G)$. The result follows from $\mathfrak{so}(3) \cong \mathfrak{sl}(2)$. \square

Remark 7.8. For the $\text{Br}^{-Q^{1/2}}$ expansion of the S -polynomial, at $Q = 4$ the binor identity implies that the extension of the S -polynomial to accommodate half twists with  has the property that the insertion of a half twist multiplies the polynomial by -1 . Thus $S_G(4) = \pm F_G(4)$ whether or not G has this sort of half twist (which are presumed to be ignored by F).

7.4. Cellular embedding polynomial. Recall the other formulation of $W_{\mathfrak{sl}(N)}(G)$ when G is a

cubic graph, where vertices are replaced by  -  and edges by . As suggested in [3],

by thinking of  and  as being two rotations for a vertex, we can identify the coefficient of N^{2k} in $W_{\mathfrak{sl}(N)}(G)$ as a signed count of the number of genus- $(b_0(G) + \frac{1}{4}|V(G)| - k)$ virtual graphs with the same underlying graph as G , with the sign being determined by the parity of the number of vertices with opposite rotation. With the normalization in Lemma 7.4, the coefficient of N^{2k} is for the genus- $(b_0(G) + \frac{1}{2}|V(G)| - k)$ virtual graphs.

With the Lemma 7.4 normalization, the evaluation $C_G(x) = x^{1+\frac{1}{2}|V(G)|} W_{\mathfrak{sl}(x^{-1/2})}(G)$ is a polynomial such that the coefficient of the x^g term is instead for the genus- $(g - b_0(G) + 1)$ virtual graphs, and we call it the *cellular embedding polynomial*. A restatement of Lemma 7.5 is that the underlying graph of a cubic virtual graph G is planar if and only if $C_G(0) \neq 0$.

Consider the polynomial invariant p of virtual graphs such that $p_G(x) = x^{g(G) - b_0(G) + 1}$. For $e \in E(G)$, if e is not a loop then $p_G(x) = p_{G/e}(x)$. Otherwise, the cellular embedding $G \hookrightarrow \Sigma$ decomposes as a connect sum $\Sigma = \Sigma_1 \# \Sigma_2$ along e , so $p_G(x) = p_{G/e}(x)$ as well since $g(\Sigma) = g(\Sigma_1) + g(\Sigma_2)$ and $b_0(\Sigma) = b_0(\Sigma_1) + b_0(\Sigma_2) - 1$. The last rule that specifies $p_G(x)$ is that if G is a union of k isolated vertices, $p_G(x) = x^{k-1}$.

We can write $C_G(x) = \sum_{W \in V(G)} (-1)^{|W|} p_{\sigma_W(G)}(x)$ for cubic G . Since it is related to $W_{\mathfrak{sl}(N)}$, it shares many properties such as multiplicativity (up to a factor) under edge connect sum and vertex connect sum, as well as satisfying the IHX relation.

One can define a kind of “nonplanar” algebra for p by taking as elements compact surfaces with boundary subdivided into labeled arcs, with the relation that $[\Sigma \# T^2] = x[\Sigma]$, and with a map from cubic virtual graphs by sending cubic vertices to a difference of two triangles with opposite orientations. The second author calculated the cellular embedding polynomial in this way for all connected cubic graphs with up to 22 vertices and girth at least 3. There are 471,932 such polynomials, 684 of which are for planar graphs. Of the planar graphs, the nearest roots to $1/4$ are real, and the nearest occurs in $2(1 - x)(1 + 16x + 87x^2 - 504x^3 + 368x^4)$, the S -polynomial of a graph with 22 vertices.

8. YAMADA POLYNOMIAL

Yamada introduced a one-variable Laurent polynomial invariant $R_G(q)$ for spatial graphs G in [24]. It is the $\mathcal{U}_q(\mathfrak{sl}_2)$ Reshetikhin-Turaev invariant of cubic spatial graphs, coloring the edges with the 3-dimensional irreducible representation V_2 , placing the intertwiner $V_2 \otimes V_2 \rightarrow V_2$ at vertices, and extending to arbitrary degree through contraction-deletion.

There are a few normalizations of $R_G(q)$ in the literature, and we choose one implicitly in the following definition, differing by a factor of $(-1)^{|V(G)|-|E(G)|}$ from the original:

Definition 8.1. Let G be a spatial graph. The Laurent polynomial $R_G(q)$ is determined by the following properties:

- (1) If G has a diagram with no (classical) crossings, then

$$R_G(q) = F_G((q^{1/2} + q^{-1/2})^2),$$

where F_G is the flow polynomial of this diagram.

- (2) There is the following local relation:

$$\bigotimes_q = q \bigcirc \bigcirc_q + q^{-1} \bigotimes_q - \bigotimes \bigotimes_q,$$

where all four disks represent diagrams that differ only within the disk in the way represented, and where G_q is shorthand for $R_G(q)$.

One may evaluate the Yamada polynomial of a spatial graph whose diagram has n crossings by expanding all the crossings with the local relation to get 3^n planar graphs, and then evaluating the flow polynomial for each expansion.

If G is a cubic flat vertex graph, then $R_G(q)$ is well-defined up to a power of q^2 . If it is merely a cubic pliable vertex graph, then it is well-defined up to a power of $-q$. Thus, if G is pliable isotopic to a planar graph, $R_G(q) = (-q)^k F_G((q^{1/2} + q^{-1/2})^2)$, for some power of k .

There is an extension of the Yamada polynomial to virtual spatial graphs by Fleming and Mellor in [11], which we will denote by $R_G^F(q)$, where the flow polynomial is used for the expansions. This polynomial has the weakness that it is unable to distinguish the graphs in Figure 5. We suggest a different extension of the Yamada polynomial for virtual spatial graphs that is, however, able to distinguish these graphs. This is essentially a quantum virtual link invariant as Kauffman defined it in [13], but for virtual spatial graphs.

Definition 8.2. Let G be a virtual spatial graph. The Laurent polynomial $R_G^S(q)$ is determined by the following properties:

- (1) If G is a virtual graph (that is, if there is a diagram for G with no classical crossings), then

$$R_G^S(q) = S_G((q^{1/2} + q^{-1/2})^2),$$

where S_G is the S -polynomial of this diagram.

- (2) There is the following local relation:

$$\bigotimes_q = q \bigcirc \bigcirc_q + q^{-1} \bigotimes_q - \bigotimes \bigotimes_q$$

with the same convention as in Definition 8.1, but with R^S instead of R .

This is an invariant because the S -polynomial is locally the flow polynomial and because the Yamada polynomial is an invariant. That is, the virtual crossings can be “moved” away from the region where a Reidemeister or rigid vertex isotopy move occurs. Virtual graph moves come for free from the definition of S_G . Well-definedness can be observed by writing out a state sum, or by thinking about the local relation as corresponding to an expansion in the Brauer category.

We can use the polynomials together to extend [19, Proposition 5.1] to all virtual spatial graphs, rather than just virtual links:

Theorem 8.3. *If G is a virtual spatial graph and $R_G^F(q) \neq R_G^S(q)$, then G is not equivalent to a classical spatial graph. If G is additionally cubic, then if $R_G^F(q) \neq R_G^S(q)$, then G is not pliable vertex isotopy equivalent to a classical spatial graph.*

Proof. If G were equivalent to a classical spatial graph, both of these polynomials would coincide with $R_G(q)$. In the case G is cubic, both R^F and R^S have the same relations for pliable vertex isotopy as does R , and so both sides accumulate the same number of factors of $-q$ in a sequence of pliable vertex isotopy moves. \square

Example 8.4. For example, if G is the toroidal theta graph in Figure 5,

$$\begin{aligned} R_G^F(q) &= (q + q^{-1})(q + 1 + q^{-1}) \\ R_G^S(q) &= -2(q + 1 + q^{-1}), \end{aligned}$$

so G is not pliable vertex isotopy equivalent to a classical spatial graph. Note also that R^F is the same for both theta graphs.

Example 8.5. Consider D from [13] (see Figure 18), a virtual knot with trivial virtual Jones polynomial that Kauffman’s Z refinement was unable to tell whether or not was classical.

$$\begin{aligned} R_D^F(q) &= q^2(q + 1 + q^{-1}) \\ R_D^S(q) &= -(q - 1 - q^{-1})(q^2 + q - q^{-1})(q + 1 + q^{-1}). \end{aligned}$$

Example 8.6. The virtual knot K in Figure 19 has $R_K^F(q) = R_K^S(q) = q + 1 + q^{-1}$. K is nonclassical [13], hence Theorem 8.3 is not a necessary condition for non-classicality, and there are nontrivial virtual knots with the same R^F and R^S polynomials as the unknot’s.

Example 8.7. If U is the unlink of two circles, $R_U^F(q) = R_U^S(q) = (q + 1 + q^{-1})^2$. If L is the “virtual unlink” in Figure 20,

$$\begin{aligned} R_L^F(q) &= -(q + 1 + q^{-1}) \\ R_L^S(q) &= (q + 1 + q^{-1})^2, \end{aligned}$$

hence R^F can distinguish L from U , even up to framing. Paired with the theta graph example, we see that neither R^F nor R^S is a finer invariant than the other.

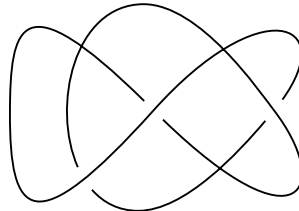


FIGURE 18. Virtual knot D from [13] with trivial virtual Jones polynomial.

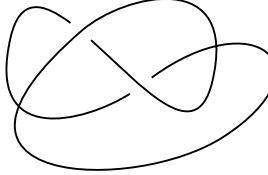


FIGURE 19. A virtual knot of virtual genus 1 for which Theorem 8.3 cannot detect non-classicality.

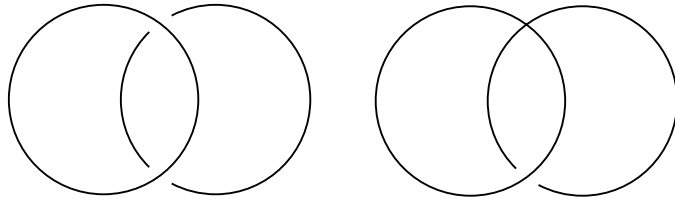


FIGURE 20. Unlink and “virtual unlink,” distinguishable by R^F and not R^S .

Remark 8.8. This theorem gives an algebraic proof of a weaker form of Corollary 2.5: if G is a virtual graph with no bridge edges, then while Theorem 6.12 implies $\deg S_G(Q) = b_1(G) - g(G)$, it is well known that $\deg F_G(Q) = b_1(G)$, so if $g(G) \neq 0$, Theorem 8.3 implies that the virtual genus of G as a virtual spatial graph is not zero.

Theorem 8.9. *If G is a virtual spatial graph, $R_G^F(-1) = R_G^S(-1) = F_G(0) = S_G(0)$, where classical crossings are ignored for F and S . If G is cubic, $F_G(4) = R_G^F(1) = \pm R_G^S(1)$ and $R_G^S(1) = \pm S_G(4)$.*

Proof. At $q = \pm 1$, the ninety-degree rotational symmetry of the right-hand sides of the local relations for both Yamada polynomials gives $\bigotimes_q = \bigotimes_q$. At $q = -1$, since $(q^{1/2} + q^{-1/2})^2 = 0$, both Yamada polynomials involve evaluations of the flow and S -polynomials at 0, hence $R_G^F(-1) = R_G^S(-1)$. Every virtual spatial graph, up to virtual pliable vertex isotopy and crossing interchange, is equivalent to a virtual graph. Since R^F at $q = -1$ is invariant under both types of moves, $R_G^F(-1) = F_G(0)$, where the flow polynomial is of the underlying graph, and we previously showed $F_G(0) = S_G(0)$.

Similarly, at $q = 1$ we have $R_G^F(1) = F_G(4)$. $R_G^S(1)$ is invariant under crossing interchange, but it becomes negative with cubic vertex flips. If we perform a sequence of such moves to represent G as a virtual graph, we have $R_G^S(1) = \pm S_G(4)$. \square

ACKNOWLEDGEMENTS

We would like to thank Noah Snyder for helpful advice and for introducing us to the connection between diagrams on surfaces and virtual crossings, Slava Krushkal for the suggestion to study chromatic identities for surface graphs, and Paul Fendley for encouragement.

REFERENCES

- [1] Ian Agol and Vyacheslav Krushkal, *Tutte relations, TQFT, and planarity of cubic graphs*, Illinois Journal of Mathematics **60** (2016), no. 1, 273–288, arXiv:1512.07339v1 [math.CO]. MR 3665181
- [2] Martin Aigner, *The Penrose polynomial of a plane graph*, Mathematische Annalen **307** (1997), no. 2, 173–189. MR 1428870
- [3] Dror Bar-Natan, *Lie algebras and the four color theorem*, Combinatorica **17** (1997), no. 1, 43–52, arXiv:q-alg/9606016v1. MR 1466574
- [4] Béla Bollobás and Oliver Riordan, *A polynomial invariant of graphs on orientable surfaces*, Proc. London Math. Soc. (3) **83** (2001), no. 3, 513–531. MR 1851080
- [5] Richard Brauer, *On algebras which are connected with the semisimple continuous groups*, Ann. of Math. (2) **38** (1937), no. 4, 857–872. MR 1503378

- [6] J. Scott Carter, Seiichi Kamada, and Masahico Saito, *Stable equivalence of knots on surfaces and virtual knot cobordisms*, J. Knot Theory Ramifications **11** (2002), no. 3, 311–322, arXiv:math/0008118v1. MR 1905687
- [7] Sergei Chmutov, *Generalized duality for graphs on surfaces and the signed Bollobás-Riordan polynomial*, J. Combin. Theory Ser. B **99** (2009), no. 3, 617–638, arXiv:0711.3490v3 [math.CO]. MR 2507944
- [8] S. V. Duzhin, A. I. Kaishev, and S. V. Chmutov, *The algebra of 3-graphs*, Tr. Mat. Inst. Steklova **221** (1998), 168–196. MR 1683693
- [9] Joanna A. Ellis-Monaghan and Iain Moffatt, *A Penrose polynomial for embedded graphs*, European Journal of Combinatorics **34** (2013), no. 2, 424–445. MR 2994409
- [10] Paul Fendley and Vyacheslav Krushkal, *Tutte chromatic identities from the Temperley-Lieb algebra*, Geom. Topol. **13** (2009), 709–741, arXiv:0711.0016v3. MR 2469528
- [11] Thomas Fleming and Blake Mellor, *Virtual spatial graphs*, Kobe J. Math. **24** (2007), no. 2, 67–85, arXiv:math/0510158v2. MR 2488753
- [12] Jesper Lykke Jacobsen and Jesús Salas, *A generalized Beraha conjecture for non-planar graphs*, Nuclear Phys. B **875** (2013), no. 3, 678–718, arXiv:1303.5210v2. MR 3102902
- [13] Louis H. Kauffman, *Virtual knot theory*, European Journal of Combinatorics **20** (1999), no. 7, 663–690. MR 1721925
- [14] Louis Hirsch Kauffman and Vassily Olegovich Manturov, *Graphical constructions for the $sl(3)$, C_2 and G_2 invariants for virtual knots, virtual braids and free knots*, Journal of Knot Theory and its Ramifications **24** (2015), no. 6, 1550031, 47. MR 3358442
- [15] Oliver King, Paul Martin, and Alison Parker, *On central idempotents in the Brauer algebra*, September 2016, arXiv:1609.01183v1.
- [16] Vyacheslav Krushkal, *Graphs, links, and duality on surfaces*, Combin. Probab. Comput. **20** (2011), 267–287, arXiv:0903.5312v3. MR 2769192
- [17] Greg Kuperberg, *What is a virtual link?*, Algebraic & Geometric Topology **3** (2003), 587–591. MR 1997331
- [18] Gustav Lehrer and Ruibin Zhang, *The second fundamental theorem of invariant theory for the orthogonal group*, Annals of Mathematics. Second Series **176** (2012), no. 3, 2031–2054. MR 2979865
- [19] Yasuyuki Miyazawa, *The Yamada polynomial for virtual graphs*, Intelligence of low dimensional topology 2006, Ser. Knots Everything, vol. 40, World Sci. Publ., Hackensack, NJ, 2007, pp. 205–212. MR 2371727
- [20] Roger Penrose, *Applications of negative dimensional tensors*, Combinatorial Mathematics and its Applications (Proc. Conf., Oxford, 1969), Academic Press, London, 1971, pp. 221–244. MR 0281657
- [21] N. Y. Reshetikhin and V. G. Turaev, *Ribbon graphs and their invariants derived from quantum groups*, Comm. Math. Phys. **127** (1990), no. 1, 1–26. MR 1036112
- [22] Imre Tuba and Hans Wenzl, *On braided tensor categories of type BCD*, Journal für die Reine und Angewandte Mathematik. [Crelle’s Journal] **581** (2005), 31–69. MR 2132671
- [23] Hans Wenzl, *On the structure of Brauer’s centralizer algebras*, Ann. of Math. (2) **128** (1988), no. 1, 173–193. MR 951511
- [24] Shuji Yamada, *An invariant of spatial graphs*, Journal of Graph Theory **13** (1989), no. 5, 537–551. MR 1016274

DEPARTMENT OF MATHEMATICS, UNIVERSITY OF CALIFORNIA, BERKELEY, CALIFORNIA 94720
E-mail address: cmcs@math.berkeley.edu

DEPARTMENT OF MATHEMATICS, UNIVERSITY OF CALIFORNIA, BERKELEY, CALIFORNIA 94720
E-mail address: kmill@math.berkeley.edu